

TWENTYFIFTH EUROPEAN ROTORCRAFT FORUM

Paper n° G18

STABILIZATION OF A BLADE WITH A SEVERED PITCH LINK
USING A TRAILING EDGE FLAP

BY

ROBERTO CELI
UNIVERSITY OF MARYLAND, COLLEGE PARK, USA

SEPTEMBER 14-16, 1999
ROME
ITALY

ASSOCIAZIONE INDUSTRIE PER L'AEROSPAZIO, I SISTEMI E LA DIFESA
ASSOCIAZIONE ITALIANA DI AERONAUTICA E ASTRONAUTICA

STABILIZATION OF A BLADE WITH A SEVERED PITCH LINK USING A TRAILING EDGE FLAP

Roberto Celi¹

Department of Aerospace Engineering
Glenn L. Martin Institute of Technology
University of Maryland, College Park, USA

Introduction

Abstract

This paper addresses the feasibility of using trailing edge flaps to reconfigure a helicopter rotor blade following a failure of the pitch link, which makes the blade free-floating in pitch and otherwise uncontrollable. A coupled rotor-fuselage model is developed which allowed for rotor anisotropy. A new, optimization-based, trim procedure is developed to determine the dynamics of the failed blade, and the flap inputs required for reconfiguration. The trailing edge flap appears capable of correcting the otherwise catastrophic consequences of a pitch link failure. The residual 1/ and 2/rev components of the hub loads appear to be reasonably small. The flap acts by generating a rigid-body pitching motion of the free-floating blade that matches the angles that otherwise would have been generated by the swashplate. The steady-state flapping motion of the reconfigured blade is very nearly identical to those of the undamaged blades. Therefore, if a helicopter rotor is equipped with trailing edge flaps for other purposes such as vibration or noise reduction, these flaps could be used as emergency control surfaces.

Notation

S	Descent direction in optimization procedure for trim
X	Vector of design variables in trim procedure
β	Blade flapping angle
δ_F	Flap deflection
μ	Advance ratio
ψ	Azimuth angle of the reference blade (blade number 1)
ϕ	Rigid body pitch of the failed blade
Ω	Rotor speed

Subscripts and superscripts

$()_{nc}$	cosine component of n -th harmonic
$()_{ns}$	sine component of n -th harmonic
$()_4$	Quantity for blade number 4 (failed blade)
$()^4$	Quantity for blade number 4 (failed blade)

In recent years there has been a renewed interest in the use of trailing edge flaps on the main rotor blades for noise and vibration reduction. Extensive theoretical research has been carried out, and model scale tests have been performed. Full-scale experimentation is now under way.

Trailing edge flaps provide additional control effectors, besides the conventional swashplate controls. Therefore, they offer some degree of control redundancy, and could potentially be used to reconfigure the rotor control chain in case of failures. Control reconfiguration has been successfully explored and tested in fixed-wing applications. On the other hand, the potential for helicopter applications has been severely limited by the lack of control redundancy, as shown by the few studies on this topic.

Aponso *et al.* [1] have studied a case in which the roll swashplate actuator of a Sikorsky UH-60 is jammed or floating. No additional control surfaces were assumed, and reconfiguration was carried out through changes in the flight control laws. A simple linearized aircraft model was used. Huang *et al.* [2] have considered a CH-47 tandem rotor configuration with combinations of jammed front and rear swashplate actuators. Reconfiguration was achieved through changes in the flight control laws. In one of the cases studied some control redundancy was obtained by assuming that the rotational speeds of the rotors could be varied by up to $\pm 10\%$. A simple linearized 6-DOF analysis model was used. In the only other published study on this topic, Heiges [3] has considered a configuration representative of the AH-64 with all the pitch links severed. Control was restored through the use of servo-flaps installed on all the blades. The study was based on a simple linearized rotor analysis.

The main objective of this paper is to study the dynamics and the reconfiguration of a single main rotor helicopter in which the pitch link of one of the blades has been severed, so that the blade is free-floating in pitch. The reconfiguration is achieved through the use of a trailing edge flap. The blade is schematically shown in Figure 1. The specific problem that will be addressed is whether one can determine a flap control history that: (i) allows the trimming of the failed rotor, and (ii) reduces the hub loads to acceptable levels. Because the focus of the study is simply to establish the theoretical feasibility of this type of reconfiguration, the control considered in this study is open-loop only, and no feedback is considered.

The mathematical model is much more detailed than in the studies mentioned above. It includes a full nonlinear, coupled rotor-fuselage dynamic model, from which

¹Associate Professor, Alfred Gessow Rotorcraft Center; e-mail: celi@eng.umd.edu.

a linearized, time-varying model can also be extracted. The anisotropy of the rotor, which has one blade with a dynamics different from that of the other three, is fully taken into account. A new trim procedure is presented; the new procedure is required to deal with the rotor anisotropy and the flap control history.

Baseline simulation model

The mathematical model of the helicopter used in this study is a nonlinear blade element type model that includes fuselage, rotor, and main rotor inflow dynamics. The 6 degree of freedom rigid body motion of the aircraft is modeled using nonlinear Euler equations. Linear aerodynamics is assumed for fuselage and empennage. The blades are assumed to be rigid, with offset hinges and root springs. Flap and lag dynamics of each blade are modeled. The main rotor has four blades.

The coupled system of rotor, fuselage, and inflow equations of motion is written in first-order form. The state vector has a total of 28 elements: flap and lag displacements and rates for each of the 4 blades (16 states); 9 rigid body velocities, rates, and attitudes; and 3 inflow states.

In the absence of a failure, the trim procedure is the same as in Ref. [4]. Thus, the rotor equations of motion are transformed into a system of nonlinear algebraic equations using a Galerkin method. The algebraic equations enforcing force and moment equilibrium are added to the rotor equations, and the combined system is solved simultaneously. The solution yields the harmonics of a Fourier series expansion of the rotor degrees of freedom, the pitch control settings, the trim attitudes and rates of the entire helicopter, and the main and tail rotor inflow.

Modeling of the failed blade

The blade with the severed pitch link is assumed to be free-floating in pitch as a rigid body. The flap and lag dynamic model remains otherwise unchanged. The inertia moments due to the motion of the flap are neglected. Therefore, the pitch equation of motion is simply:

$$\ddot{\phi} + \Omega^2 \phi = M_\phi \quad (1)$$

where Ω is the rotor speed and M_ϕ is the nondimensional aerodynamic pitching moment. The only aerodynamic pitching moment is that generated by the deflection of the trailing edge of the flap. The flap deflection $\delta_F(\psi)$, is assumed to have a harmonic variation, that is:

$$\delta_F(\psi) = \delta_0 + \sum_{n=1}^N (\delta_{nc} \cos n\psi + \delta_{ns} \sin n\psi) \quad (2)$$

with $\delta_F > 0$ for a downward deflection of the flap. The cases $N = 1$ and $N = 2$ will be considered in the present paper. The pitching moment coefficient c_{mF} is assumed to be linearly proportional to the flap deflection, and is given by $c_{mF} = -0.64\delta_F$.

When the pitch link is severed, the swashplate pitch inputs are no longer applied to the blade. Therefore, the geometric angle of attack of the free floating blade is given by the sum of the rigid body pitch rotation ϕ and the twist angle θ_B . This angle is used to calculate all the aerodynamic forces acting on the blade (including the flap and lag dynamics).

While the pitching model of the blade is probably adequate for a feasibility study, its limitations should be kept in mind. The most serious is the lack of unsteady aerodynamic modeling. Even in the absence of a trailing edge flap, the motion of the airfoil introduces changes in both the magnitude and the phase of the lift, drag, and pitching moment coefficients; in particular, aerodynamic pitch damping is generated. The addition of the flap introduces further changes of the aerodynamic coefficients. A model such as that of Ref. [5] should be used for a more accurate representation of the unsteady aerodynamics of the flapped airfoil.

On the other hand, neglecting the elastic torsion of the free-floating blade is not likely to be a serious assumption. The changes in lead-lag dynamics can also be neglected, at least at the level of approximation used in the present study. It has been shown by Wang [6] that small dissimilarities in rotor blade dynamics tend to increase the aeroelastic stability of the rotor. Therefore, if the dynamics of the reconfigured blade is close or identical to that of the other blades, the rotor should at least maintain the level of stability that it had before the failure.

In summary, the coupled rotor-fuselage mathematical model consists of 30 nonlinear ODE, namely: 9 Euler equations for rigid body motion, 3 dynamic inflow equations, 2 equations for the flap and 2 for the lag dynamics of each of the 4 blades, and 2 pitch equations for the failed blade.

Trim procedure for the rotor with a failed blade

The trim procedure of Ref. [4] needs to be modified to take into account the damage to the blade. This is necessary for two primary reasons, namely: (i) the rotor anisotropy, and (ii) the need to determine the required flap trim control.

Treatment of rotor anisotropy

The free-floating blade has a dynamics different from that of the other three blades, and therefore it needs its own separate equations in the system of algebraic trim equations. Rigid-body flap and pitch dynamics of the free-floating blade are explicitly included in the trim procedure, whereas the lag dynamics is assumed to remain unchanged in trim. The flap and the pitch angles are represented in the form of a truncated Fourier series expansion, that is:

$$\beta^4(\psi) = \beta_0^4 + \sum_{n=1}^2 (\beta_{nc}^4 \cos n\psi_4 + \beta_{ns}^4 \sin n\psi_4) \quad (3)$$

$$\phi^4(\psi) = \phi_0^4 + \sum_{n=1}^2 (\phi_{nc}^4 \cos n\psi_4 + \phi_{ns}^4 \sin n\psi_4) \quad (4)$$

where the subscripts and superscripts "4" indicate that the failed blade is the fourth, with $\psi_4 = \psi + 270^\circ$. Compared with the trim procedure of Ref. [4] there are new trim unknowns, namely the coefficients of the Fourier series above. Therefore, anisotropy adds 10 unknowns to the trim problem. The corresponding 10 additional trim equations come from the application of Galerkin method [4]. For flap they are:

$$\begin{aligned} \int_0^{2\pi} \varepsilon_{F4}(\psi) d\psi &= \int_0^{2\pi} \varepsilon_{F4}(\psi) \cos \psi d\psi = \\ &= \int_0^{2\pi} \varepsilon_{F4}(\psi) \sin \psi d\psi = \int_0^{2\pi} \varepsilon_{F4}(\psi) \cos 2\psi d\psi = \\ &= \int_0^{2\pi} \varepsilon_{F4}(\psi) \sin 2\psi d\psi = 0 \end{aligned} \quad (5)$$

where $\varepsilon_{F4}(\psi)$ is the residual obtained when the tentative trim solution is substituted into the flap equation of motion for the failed blade. Five similar equations are then written for the residual $\varepsilon_{P4}(\psi)$ of the blade pitch equation.

The total number of trim equations and unknowns for the case of the rotor with a failed blade case is 36. Besides the 10 unknowns just mentioned, the trim procedure yields values of the pitch settings of main rotor and tail rotor; fuselage angle of attack and sideslip angle; roll and pitch attitudes; roll, pitch, and yaw rates; and the harmonics of the steady-state flap and lag motions for the undamaged blades.

Determination of flap input

The coefficients δ_0 , δ_{nc} , and δ_{ns} that describe the motion of the flap (see Eq. (2)) cannot be directly added to the set of trim unknowns, because there are no corresponding algebraic equations. Therefore, the trim formulation would consist of more unknowns than equations, and an infinite number of trim states would then exist.

The solution devised for this study is to insert the baseline trim procedure in an unconstrained optimization loop. The vector \mathbf{X} of design variables of the optimization consists of the coefficients of the flap motion:

$$\mathbf{X}^T = [\delta_0 \delta_{1c} \dots \delta_{nc} \delta_{1s} \dots \delta_{ns}] \quad (6)$$

Because the rotor is now anisotropic, multiblade load cancellations will not occur, and all harmonics of the hub loads will generally be present. If the generic hub force or moment component f is written in the form

$$f(\mathbf{X}) = f_0 + \sum_{n=1}^2 (f_{nc} \cos n\psi + f_{ns} \sin n\psi) \quad (7)$$

the objective function to be minimized is

$$F(\mathbf{X}) = \left\{ \sum_{m=1}^6 \sum_{n=1}^2 [(f_{nc}^2)_m + (f_{ns}^2)_m] \right\}^{1/2} \quad (8)$$

where the subscript m denotes each of the three hub force and three hub moment components. In other words, the optimization loop attempts to minimize the coefficients of the 1/rev and 2/rev harmonics of all six hub components.

The resulting problem can be solved using any unconstrained minimization algorithm. In the present study the Fletcher-Reeves conjugate gradient algorithm [7] is used. Therefore, the improved value of the flap motion vector \mathbf{X}_{k+1} is given by:

$$\mathbf{X}_{k+1} = \mathbf{X}_k + \alpha^* \mathbf{S}_k \quad (9)$$

where α^* denotes the minimum of $F(\mathbf{X})$ along the direction \mathbf{S}_k , which is obtained from

$$\begin{aligned} \mathbf{S}_k &= -\nabla F(\mathbf{X}_k) + \beta \mathbf{S}_{k-1} \\ \text{with } \beta &= \frac{\nabla F^T(\mathbf{X}_k) \nabla F(\mathbf{X}_k)}{\nabla F^T(\mathbf{X}_{k-1}) \nabla F(\mathbf{X}_{k-1})} \end{aligned} \quad (10)$$

where k denotes the iteration number and $\beta = 0$ for $k = 1$. Note that, for every value of $F(\mathbf{X})$ required during the optimization, a complete trim calculation is performed. The final solution consists of the vector \mathbf{X} that minimizes the sum of the absolute values of all the components of the 1/rev and 2/rev hub loads plus the corresponding values of all the trim variables.

Results

The results presented in this section refer to a soft-in-plane, hingeless rotor helicopter configuration roughly similar to a BO-105. The chordwise extension of the flap is 20% of the blade chord. The flap extends over the outermost 20% of the blade.

Figure 2 shows the iteration history of the objective function of the new trim procedure, i.e., the RMS value of the 1/rev and 2/rev components of the hub loads at an advance ratio $\mu = 0.15$. One iteration is defined as the calculation of one direction of descent \mathbf{S}_k , Eq. (10), and a one-dimensional minimization along \mathbf{S}_k to obtain the new vector of flap coefficients \mathbf{X}_{k+1} , Eq. (9). The direction finding problem requires the calculation of the gradient of the objective function, and therefore 4 function evaluations for the 1-harmonic flap input. The one-dimensional minimization requires another two function evaluations besides the baseline to calculate an initial quadratic approximation. The minimum of the approximation is the candidate 1-D minimum, and replaces the point with the highest value of the objective in the updated approximation. In all the results of the present study no more than three function evaluations were needed to achieve convergence on the 1-D minimum. Therefore, each iteration of the optimization-based trim procedure required a total of between 8 and 10 evaluations of the objective function $F(\mathbf{X})$, Eq. (8). The initial guess for \mathbf{X} in Fig. 2 is a zero vector, corresponding to an inactive flap. The trim procedure clearly

converges quickly, and reduce the hub loads by almost two orders of magnitude within the first iteration.

The top part of Figure 3 shows the absolute values of the components of the 1/rev and 2/rev hub loads with the flap inactive; the bottom part shows the components with the flap activated, for the final iteration of the trim procedure. The advance ratio is again $\mu = 0.15$. All components should be equal to zero for a four-bladed rotor with identical blades and intact pitch links. Both sets of data refer to trimmed configurations. However, it is clear that for the rotor with the failed blade "trim" is just a mathematical statement, because the very large vibratory loads would quickly destroy the aircraft. The improvement brought about by the trailing edge flap is dramatic: the peak values are reduced by almost three orders of magnitude.

The objective function is plotted in Fig. 4 as a function of advance ratio. Recall that the objective function is the square root of the sum of the squares of the first and second harmonics of the six hub load components, Eq. (8). Although the residual loads increase almost quadratically with advance ratio, the flap clearly manages to contain them within reasonable limits.

The harmonics of the required flap motion are shown in Fig. 5 as a function of advance ratio. There is a constant, upward deflection of the flap of magnitude between 18.5 and 22 degrees, depending on speed. Smaller first harmonic motions are superimposed to it; their magnitudes are almost exactly zero at hover (a small amount of cyclic is needed in hover to counteract the effects of the tail rotor) and slowly increase with speed.

The mechanism of action of the trailing edge flap is evident from the results shown in Fig. 6. The figure shows the value of collective and cyclic pitch settings as a function of advance ratio, plus the first two harmonics of the rigid body pitching motion of the free-floating blade with the flap active. The constant harmonic of the pitch motion matches almost perfectly the collective pitch at every advance ratio. The same is true for lateral cyclic pitch and first harmonic cosine, and for longitudinal cyclic pitch and first harmonic sine respectively. The second harmonics of the rigid body pitch are almost negligible. Therefore, the trailing edge flap acts in such a way that the dynamic pitch response of the blade matches the pitch angles that the swashplate controls would have generated, if the pitch link had not been severed. In retrospect, this conclusion may appear obvious. It should be noted, however, that the optimization procedure used for trim does not include directly either the pitch dynamics of the failed blade or the rotor pitch settings. The match between the two types of quantity is a by-product of the attempt to minimize the 1/rev and 2/rev loads in the nonrotating system.

Because the action of the flap mimics almost perfectly the effect of the swashplate controls, the flap dynamics of the reconfigured blade is essentially identical to those of the undamaged blades. This is clearly shown in Fig. 5,

which compares the first two harmonics of the flapping motion for both types of blades. Changes in lead-lag dynamics are neglected in this study, because the drag coefficient is assumed to be constant, and not affected by the flap motion. A more realistic flap model would have to take this effect into account: drag changes will likely introduce 1/rev (and higher) lead-lag oscillations.

Figures 8 through 10 show the hub load components with the largest nondimensional values of unbalanced harmonics. Figure 8 shows the first and second harmonics of the roll moment as a function of advance ratio. The roll moment is nondimensionalized by dividing it by the roll moment of inertia of the helicopter. These harmonics are all equal to zero for the undamaged rotor. The figure shows that the 1/rev and 2/rev harmonics are almost cancelled by the flap, with the exception of the 1/rev sine component, which turns out to be the largest unbalanced component among all hub loads. The 1/rev and 2/rev harmonics of the pitching moment are shown in Fig. 9, which is drawn in the same scale as Fig. 8. The pitching moment of inertia of the helicopter is used for the nondimensionalization. The 1/rev sine and cosine harmonics have about the same size, whereas the 2/rev components are negligible. The pitch 1/rev components are the next largest hub load components. Figure 10 shows the harmonics of the Z-force, nondimensionalized using the weight of the helicopter. For this hub load component it is the 1/rev portion to be negligible, whereas the 2/rev portion has the larger harmonics, which progressively increase with advance ratio.

Including a second harmonic in the trailing edge flap input has a negligible effect. This can be seen in Fig. 4, where the objective function is plotted as a function of advance ratio for the case of 1- and 2-harmonic flap input. As expected, adding a second harmonic reduces the value of the objective function at all advance ratios, but the improvement is negligible. The magnitude of the second harmonic input is never larger than 0.011 degrees. However, it should be kept in mind that a more sophisticated aerodynamic model will probably introduce a stronger higher harmonic forcing. As a consequence, higher harmonic flap inputs may also be required.

Figure 12 shows the coupled rotor-fuselage poles for the baseline and the failed configurations, and the latter with the trailing edge flap active and inactive. The top plot contains all the poles, the bottom plot only those closest to the origin. Perhaps unexpectedly, the poles are not dramatically changed by the blade failure. In particular, the pitch link failure does not trigger any new substantial instabilities. Rather, it produces very high forced responses. The distinction is probably only of academic interest, as the aircraft would be lost without reconfiguration anyway, but it may have some repercussions on the design of the reconfiguration control laws.

Summary and Conclusions

This paper addressed the feasibility of using trailing edge flaps to reconfigure a helicopter rotor blade following a failure of the pitch link, which makes the blade free-floating in pitch and otherwise uncontrollable. The problem was studied using a coupled rotor-fuselage model which allowed for rotor anisotropy in the form of three identical blades with a fourth dissimilar one. A new, optimization-based, trim procedure was developed to determine both the dynamics of the failed (and reconfigured) blade, and the flap inputs required to achieve the best possible reconfiguration. A very simple aerodynamic model was used for the flap. While this model is adequate for a feasibility study, its limitations should be kept in mind when evaluating the conclusions of the study.

The main conclusions of the present study are:

1. The new trim procedure is effective in calculating the trim state of the helicopter with the anisotropic rotor, and in providing the stabilizing flap input.
2. The trailing edge flap is capable of correcting the otherwise catastrophic consequences of a pitch link failure. The residual 1/ and 2/rev components of the hub loads appear to be reasonably small. This is accomplished primarily through 1/rev flap inputs. The required flap deflections are high, but not unreasonably so. Adding higher harmonics to the flap input does not bring significant benefits.
3. The flap acts by generating a rigid-body pitching motion of the free-floating blade that matches at every azimuth the angles that would have been generated by the swashplate input if the pitch link had not been severed. The steady-state flapping motion of the reconfigured blade is very nearly identical to those of the undamaged blades.

The previous conclusions suggest that, if a helicopter rotor is equipped with trailing edge flaps for other purposes such as vibration or noise reduction, these flaps could be used as emergency control surfaces to help reconfigure the flight control system following a failure or battle damage.

Acknowledgments

This research was supported by the National Rotorcraft Technology Center, under the Rotorcraft Center of Excellence Program, Technical Monitor Dr. Yung Yu.

References

- [1] Aponso, B. L., Klyde, D. H., and Mitchell, D. G., "Development of Reconfigurable Flight Controls for Helicopters," Systems Technology Inc. Report STI TR-1295-1.
- [2] Huang, C. Y., Celi, R., and Shih, I.-C., "Reconfigurable Flight Control Systems for a Tandem Rotor Helicopter," *Proceedings of the 52nd Annual Forum of the American Helicopter Society*, Washington, DC, June 1996, pp. 1569-1588; to appear in the *Journal of the American Helicopter Society*.
- [3] Heiges, M., "Reconfigurable Controls for Rotorcraft — A Feasibility Study," *Journal of the American Helicopter Society*, Vol. 42, No. 3, July 1997, pp. 254-263.
- [4] Celi, R., "Hingeless Rotor Dynamics in Coordinated Turns", *Journal of the American Helicopter Society*, Vol. 36, No. 4, Oct. 1991, pp. 39-47.
- [5] Hariharan, N., and Leishman, J. G., "Unsteady Aerodynamics of a Flapped Airfoil in Subsonic Flow by Indicial Concepts," *Journal of Aircraft*, Vol. 33, No. 5, Sep.-Oct. 1996, pp. 855-868.
- [6] Wang, J. M., and Chopra, I., "Dynamics of Helicopters with Dissimilar Blades," *Proceedings of the 47th Annual Forum of the American Helicopter Society*, Phoenix, AZ, May 1991, pp. 1399-1412.
- [7] Vanderplaats, G. N., *Numerical Optimization Techniques for Engineering Design: With Applications*, McGraw-Hill, New York, 1984.

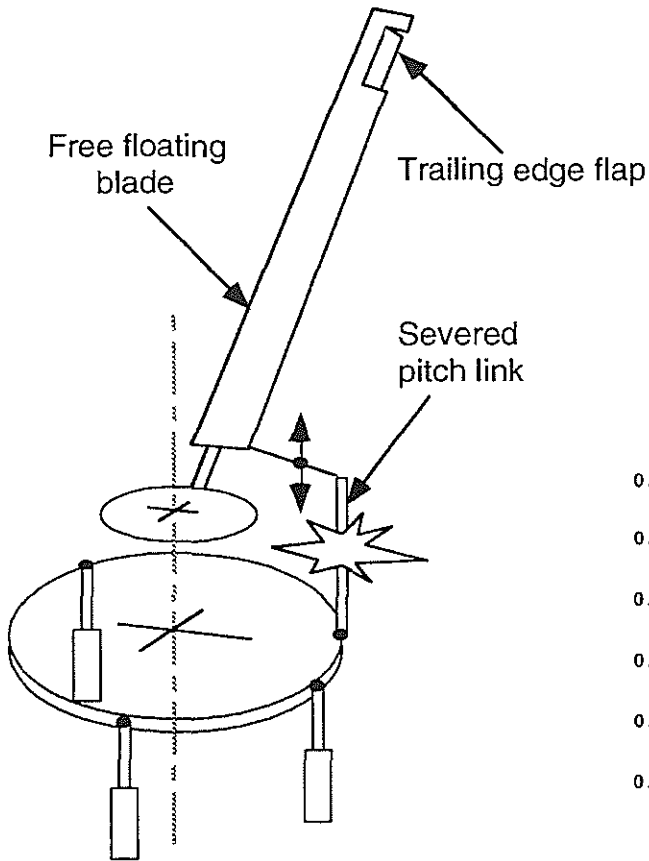


Figure 1: Blade with severed pitch link and trailing edge flap.

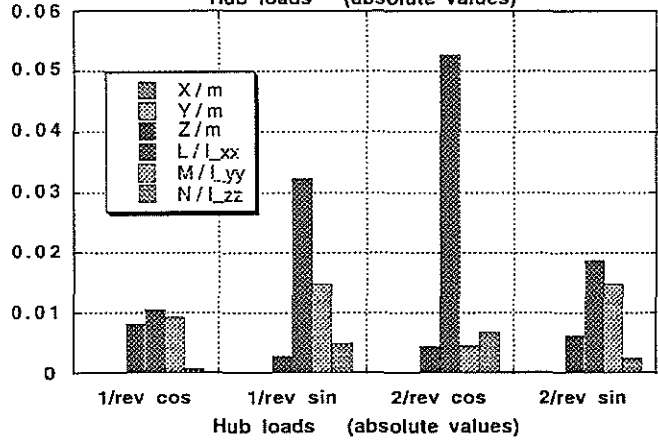
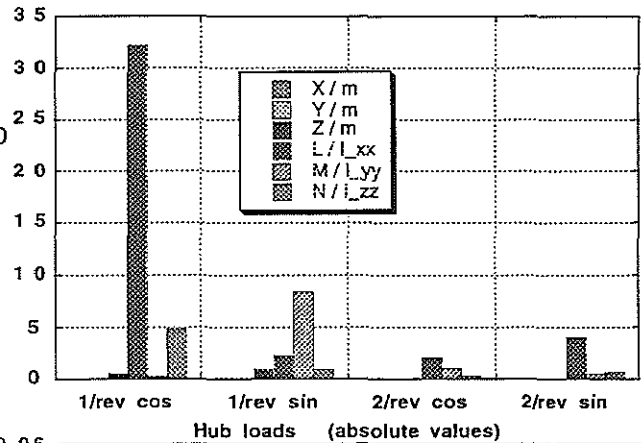


Figure 3: Components of the hub loads without flap (top) and with flap (bottom); one harmonic flap motion, $\mu = 0.15$.

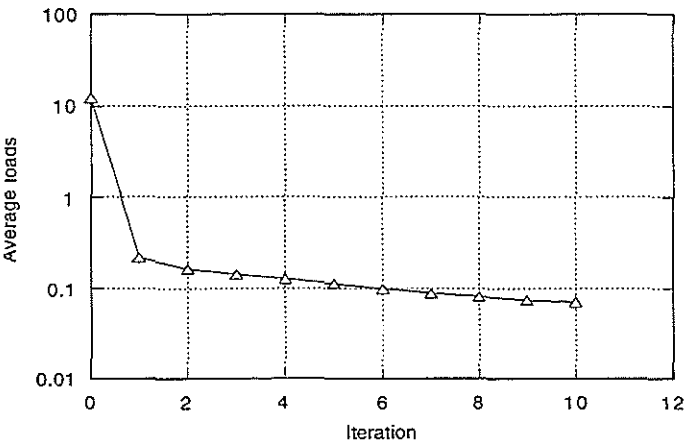


Figure 2: Iteration history of the objective function of the trim procedure; $\mu = 0.15$.

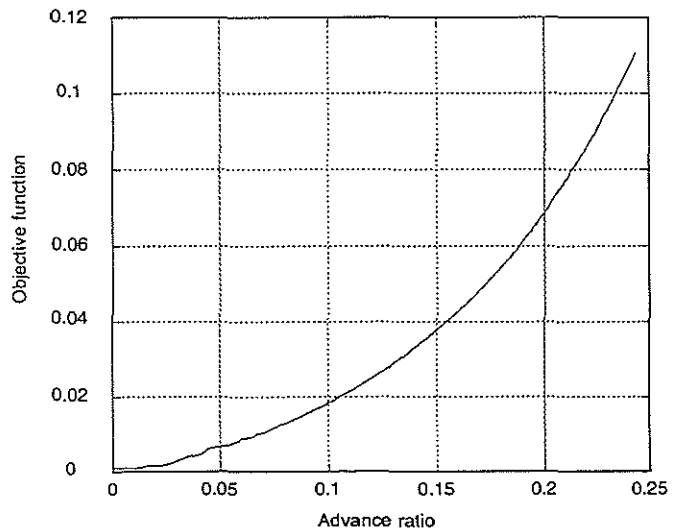


Figure 4: Objective function as a function of advance ratio.

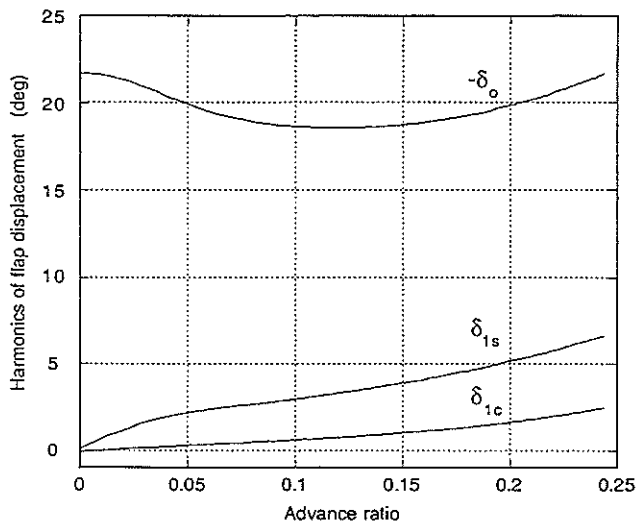


Figure 5: Harmonics of flap motion as a function of advance ratio.

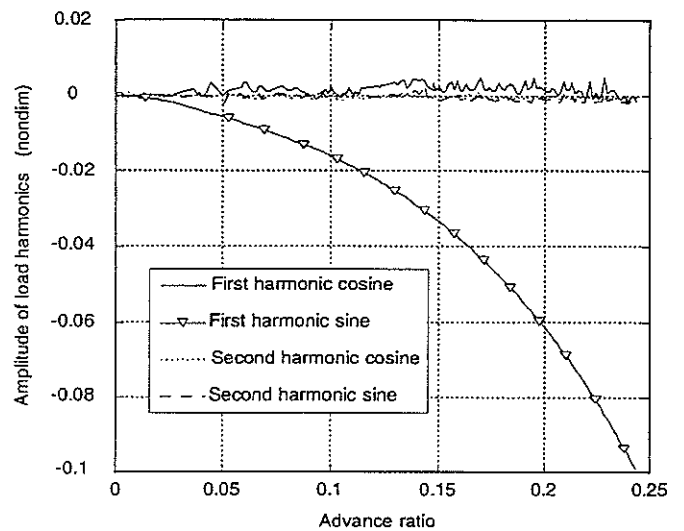


Figure 8: Harmonics of roll moment as a function of advance ratio.

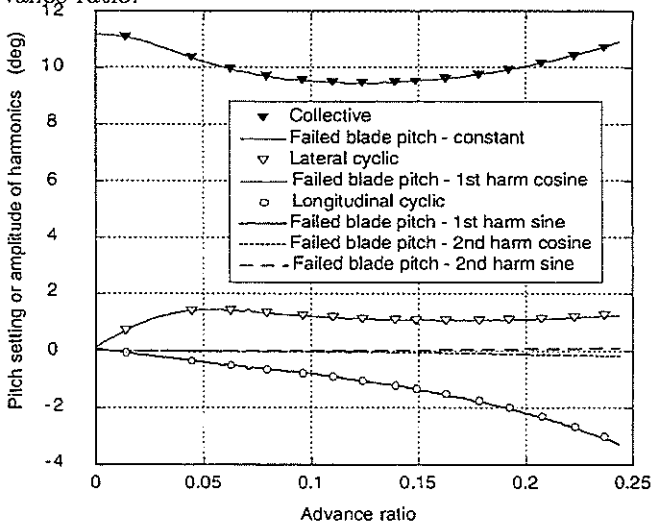


Figure 6: Pitch settings and harmonics of rigid body pitch motion of the failed blade as a function of advance ratio.

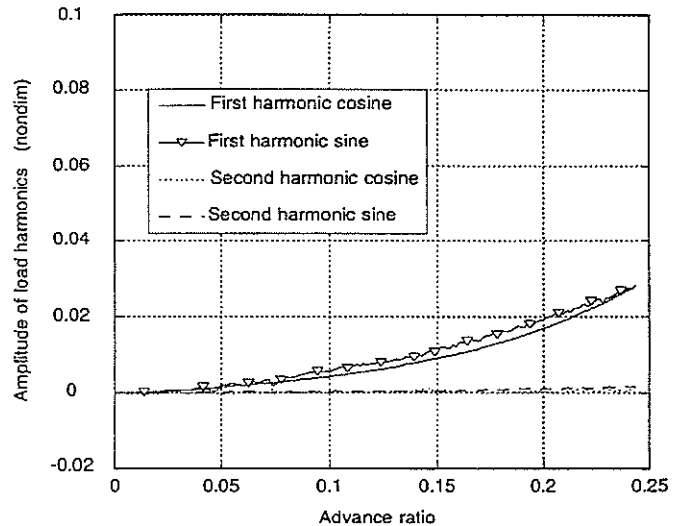


Figure 9: Harmonics of pitch moment as a function of advance ratio.

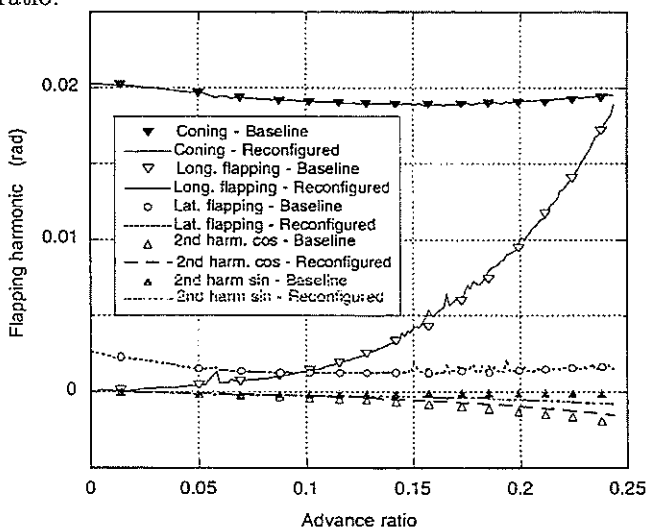


Figure 7: Flapping harmonics for baseline and reconfigured rotors as a function of advance ratio.

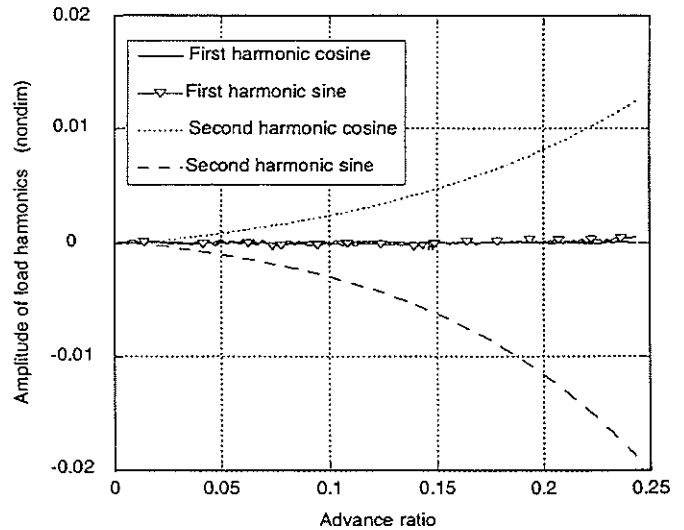


Figure 10: Harmonics of pitch moment as a function of advance ratio.

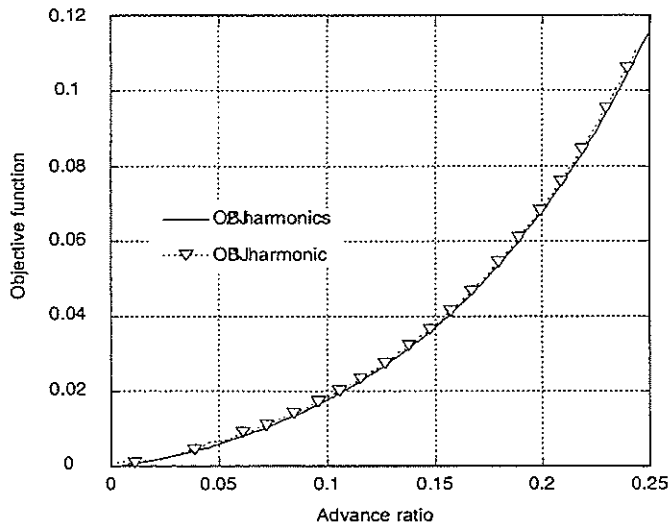


Figure 11: Objective function as a function of advance ratio for 1- and 2-harmonic flap input.

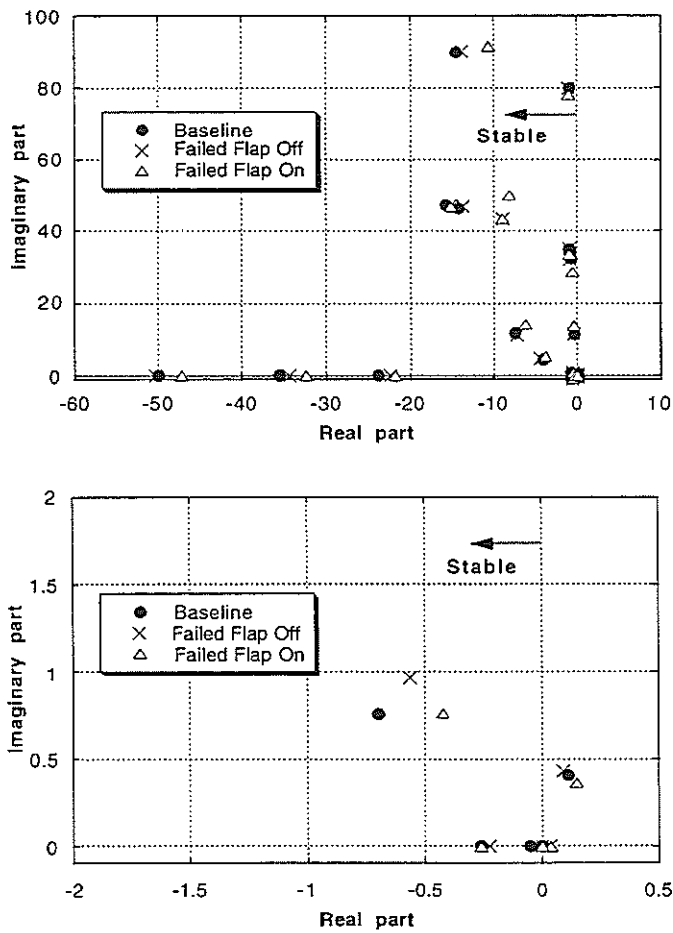


Figure 12: Coupled rotor-fuselage poles for baseline, damaged, and reconfigured rotors; advance ratio $\mu = 0.15$.